NASA TECHNICAL MEMORANDUM

NASA TM X-1376

NASA TM X-1376

FLIGHT EVALUATION OF SPLITTER-PLATE EFFECTIVENESS IN REDUCING BASE DRAG AT MACH NUMBERS FROM 0.65 TO 0.90

by Edwin J. Saltzman and John Hintz

Flight Research Center
Edwards, Calif.

NATIONAL AERONAUTICS AND SPACE ADMINISTRATION • WASHINGTON, D. C. • MAY 1967

NASA TM X-1376

FLIGHT EVALUATION OF SPLITTER-PLATE EFFECTIVENESS IN REDUCING BASE DRAG AT MACH NUMBERS FROM 0.65 TO 0.90

By Edwin J. Saltzman and John Hintz

NASA Flight Research Center
Edwards, Calif.

NATIONAL AERONAUTICS AND SPACE ADMINISTRATION

For sale by the Clearinghouse for Federal Scientific and Technical Information
Springfield, Virginia 22151 – CFSTI price $3.00

FLIGHT EVALUATION OF SPLITTER-PLATE EFFECTIVENESS IN REDUCING BASE DRAG AT MACH NUMBERS FROM 0.65 TO 0.90

By Edwin J. Saltzman and John Hintz
NASA Flight Research Center

SUMMARY

An experiment has been conducted to determine the effectiveness of a splitter plate in reducing base drag at subsonic speeds. The test configuration was a "fin-like" shape which may be representative of blunt-trailing-edge stabilizing surfaces of future hypersonic aircraft or reentry vehicles. The test chord Reynolds numbers, up to 36.2×10^6, are believed to be representative of chord Reynolds numbers for the terminal, subsonic phase of a lifting-body reentry.

The splitter plate, which extended into the wake region a distance of 1 base width, reduced the negative base pressure coefficients between 30 percent and 40 percent. This increment in base pressure coefficient was as large as obtained on a two-dimensional wind-tunnel model at the higher comparable Mach numbers and about 12 percent lower at the lower comparable Mach numbers, even though the flight results represented higher Reynolds numbers and contained outboard end (three-dimensional) effects.

INTRODUCTION

It was recognized during the earliest fluid dynamic experiments that the periodic shedding of vortices from bluff bodies was the source of much drag (incompressible laminar flow at Reynolds numbers between 60 and 5000). The importance of these periodic vortices as a source of drag resulted in Von Karman and Rubach deriving methods for computing the drag based on the momentum theorem and the geometry of the wake vortex pattern.

It was later observed that airfoils with blunt trailing edges also experienced high negative pressure coefficients over their base surfaces, even though the Reynolds numbers were too high for laminar flow and consequently too high to support a classical vortex street. It became apparent that the mere beginning of a vortex system, even with turbulent flow, would result in a significant drag penalty. Concurrently, Hoerner noted that drag coefficients obtained from aft-facing steps were lower than those for the bases of wings with blunt trailing edges. On the basis of this observation and his own experience with water-tunnel tests, he concluded that the trailing-wall surface behind aft-facing steps interfered with the formation of vortices and thus reduced the afterbody drag.

Roshko more recently studied the relationship of vortex shedding frequency and the drag of bluff bodies for incompressible flow at Reynolds numbers up to about 2×10^4 (refs. 1 to 3). He found that both Strouhal number and drag coefficient for such bodies were significantly reduced by the presence of a splitter plate in the wake (placed normal to the base surface so as to form a reattachment surface for the impinging separated flow, although reattachment does not occur for the shortest splitter plates).

It thus became apparent that the effect of the splitter plate on the periodic shedding of vortices, observed by Roshko, might be the same phenomenon as that caused by the trailing wall behind aft-facing steps, as observed by Hoerner. This in turn encouraged other investigators to study the effects of splitter plates for two-dimensional flow (refs. 4 to 10) at low to moderate Reynolds numbers and relatively low Mach numbers. The results show significant drag reductions, as great as 60 percent, for splitter plates extending 4 or more base widths aft of the base. From a practical standpoint the most interesting feature is the 30 percent to 50 percent reduction in drag that wind-tunnel tests produced for short splitter plates (1 base width in length) for turbulent flow ahead of the base.

Because such significant benefits were indicated by model tests for turbulent flow, it became of interest to determine whether comparable reductions in base drag could be achieved at the higher Reynolds numbers that may be encountered during the terminal phase of a blunt lifting-body type of reentry. Consequently, an instrumented test fixture that had a blunt base was carried beneath an F-104 airplane during a series of pilot familiarization flights. This paper presents the results of the tests which show the influence of the splitter plate on base pressure coefficient at chord Reynolds numbers to 36.2×10^6 and free-stream Mach numbers between 0.65 and 0.90. In addition, the flight data are compared with two-dimensional wind-tunnel results.

It is recognized that techniques other than the splitter plate can be employed, and often more effectively, to reduce the base drag of blunt shapes. The simple cavity, the vented cavity, variable afterbody geometry, and base bleed (sometimes referred to as mass addition) have each been investigated and show promise. The latter method (refs. 11 and 12 for subsonic applications) has been successfully applied on jet aircraft and has the advantage of also providing benefits into the supersonic Mach number range if adequate quantities of low-energy air are available.

SYMBOLS

Physical quantities are presented, where applicable, in both the International System of Units (SI) and U. S. Customary Units. Factors relating the systems are given in reference 13.

$C_{D,b}$ base drag coefficient, $\frac{D_b}{q_\infty S}$

$C_{D,0}$ zero-lift drag coefficient, $\frac{D_0}{q_\infty S}$

$\Delta C_{D,b}$ decrease in base drag coefficient attributable to splitter plate, $\frac{\Delta D_b}{q_\infty S}$

C_p base pressure coefficient, $\frac{p_b - p_\infty}{q_\infty}$ or $\frac{p_b - p_l}{q_l}$

$C_{p,b}$ base pressure coefficient for basic configuration (without splitter plate)

$C_{p,s}$ base pressure coefficient with splitter plate

$\Delta C_{p,s} = C_{p,b} - C_{p,s}$

c chord of flight-test fixture, 203 centimeters (80 inches)

D_b base drag, newtons (pounds)

D_0 zero-lift drag, newtons (pounds)

ΔD_b decrease in base drag attributable to splitter plate, newtons (pounds)

H semispan "height" of flight-test fixture, 61 centimeters (24 inches)

h width of test-fixture base, 16.3 centimeters (6.4 inches)

l length of splitter plate, i.e., distance splitter plate extends into the wake, 16.3 centimeters (6.4 inches)

M Mach number

p pressure, newtons/meter^2 (pounds/foot^2)

p_b base pressure, newtons/meter^2 (pounds/foot^2)

q dynamic pressure, $0.7M^2 p$, newtons/meter^2 (pounds/foot^2)

S reference area, meter^2 (foot^2)

Subscripts:

l referenced to local conditions ahead of base of flight-test fixture

∞ referenced to calculated free-stream conditions

TEST FACILITY

Airplane

An F-104 airplane was used in the subject experiment. It was fitted with a test panel, hereafter referred to as the flight-test fixture, shown on the aircraft in figure 1. For the flights of this experiment a portion of the ventral fin which is normally a part of the F-104 configuration was removed in order to avoid interference with the wake from the base of the flight-test fixture. The remaining portion of the ventral fin was more than 9 base thicknesses aft of the base and was far enough downstream that its influence on base pressure was negligible. A three-view drawing of the airplane with the test fixture is shown in figure 2.

Flight-Test Fixture

The flight-test fixture was originally designed and used for panel-response studies and subsequently proved to be useful for other experiments. Because the fixture has a significant base area aft of a fin-like configuration (c = 203 cm (80 in.), H = 61 cm (24 in.), h = 16.3 cm (6.4 in.)), it presented an opportunity to investigate the effectiveness of the splitter-plate concept at relatively high Reynolds numbers and at Mach numbers where compressibility begins to be a factor. Closeup views of the fixture are shown in figures 3(a) and 3(b), and a three-view drawing is presented in figure 4.

The splitter plate (see figs. 5(a) and 5(b)) was constructed of 2.28-millimeter-thick (0.09 inch) aluminum sheet reinforced with an extruded aluminum flange. The plate extended vertically from the top of the test-fixture base, where it touched the bottom surface of the airplane fuselage, to the bottom of the test-fixture base and aft into the base wake region a distance equal to the base width. An end plate (fig. 5(b)) served to stiffen the splitter-plate structure.

A notch of 0.95 centimeter ($\frac{3}{8}$ inch) radius was made in the splitter-plate structure over the base orifice so that the plate would not interfere with the orifice as a sensing port (fig. 5(b)).

Instrumentation

The primary sensors were located within the flight-test fixture. Base pressure was sensed by a pressure-electrical (strain-gage type) transducer connected to a single orifice on the base centerline 34.9 centimeters (13.75 inches) from the top of the base. Results from references 2, 4, 7, and 8 indicate that a single measurement near mid base is sufficient to define the splitter-plate pressure-coefficient increment. Local reference conditions, i.e., static pressure and local stagnation pressure, were also sensed by transducers from ports about 76 centimeters (30 inches) ahead of the base. All transducer outputs were transmitted (FM-FM) to a ground receiving station where they were translated into engineering units. Adjustments were made to the data to account for small zero shifts (tare values) that occurred between flights.

For two flight conditions (altitude = 1.53 kilometers (5000 feet), M = 0.8 and 0.9) the transducer that was sensing stagnation pressure ahead of the base went off scale (pressure was too high). Thus, for these two conditions local reference conditions were not available. The aircraft airspeed-altitude sensor display system had been calibrated, however, so all data runs were analyzed by (1) using local reference conditions ahead of the base (except for the two conditions indicated) and (2) using aircraft Mach number and applying standard-day pressures to the indicated pressure altitude and calculating a free-stream reference dynamic pressure. Analysis of the data revealed that the greatest discrepancy between these two analysis methods in the increment in base pressure coefficient attributable to the splitter plate was about 4 percent. Thus, it was deemed appropriate to present the data analyzed by both the local and free-stream reference systems.

Accuracy. – On the basis of the five flights of the experiment, the physical characteristics of the instrumentation system, and the consistency of between-flight calibrations, it is believed that pressure values from the system are accurate within ±5 percent. The basic configuration data are averaged over three flights, and the splitter-plate data are averaged over two flights, with each of the five flights including the same nine combinations of altitude and Mach number. Thus, it is estimated that the faired base pressure coefficients used to define the effectiveness of the splitter plate are accurate within ±3 percent.

TEST CONDITIONS

Of the five flights, three were made with the basic test-fixture configuration and two with the splitter plate installed (extending 1 base width into the wake region). The flights were flown in the following order:

Flight	Configuration
1	Basic
2	Splitter plate
3	Basic
4	Basic
5	Splitter plate

The nine test conditions included on each flight were as follows:

Condition	Mach number	Pressure altitude, km (ft)	Reynolds number (based on chord of fixture)
1	0.65	1.53 (5,000)	26.2×10^6
2	.75	3.36 (11,000)	25.4
3	.80	1.53 (5,000)	32.2
4	.80	3.36 (11,000)	27.0
5	.80	5.03 (16,500)	22.9
6	.85	3.36 (11,000)	28.8
7	.90	1.53 (5,000)	36.2
8	.90	3.36 (11,000)	30.4
9	.90	6.71 (22,000)	21.6

Each of the nine test conditions was maintained for an interval between $\frac{1}{2}$ minute to 1 minute to insure that transient effects and lag were avoided, that is, altitude, Mach number, and angle of attack were held constant during this period. Sideslip angles were negligible during all data runs.

RESULTS AND DISCUSSION

Base pressure coefficient data are presented in figure 6 as a function of Mach number. For figure 6(a) the static and the dynamic pressure used to compute the coefficient are based on local values of static and stagnation pressure measured ahead of the base. In figure 6(b) the base pressure coefficient is computed as a function of base pressure and free-stream static and dynamic pressures and plotted as a function of free-stream Mach number. Each part of figure 6 shows the base pressure coefficients with and without the splitter plate averaged for each flight condition over two and three flights, respectively.

Figure 7 compares the flight-test-fixture base pressure coefficients, without the splitter plate, with flight results from the bases of fins or fin-like projections of the M2-F1 lifting-body vehicle and the X-15 airplane. For the M2-F1 data (ref. 14) only vertical-fin (rudder) base pressure coefficients are considered; whereas, for the X-15 (ref. 15) results from both the fins and side fairings are included. The change in slope of base pressure coefficient with increasing Mach number for the flight-test-fixture data is typical of a wide range of body shapes. However, the level of the data from the fixture is influenced by the three-dimensionality of the fixture and, to a lesser degree, by the mutual interference between the fixture and the F-104 airplane and by Reynolds number. The same factors must necessarily influence the M2-F1 and X-15 results by varying degrees.

The effect of a splitter plate, in terms of the percentage change in base pressure coefficient, is shown in figure 8. Flight results obtained from this study are compared with two-dimensional wind-tunnel-model data. The model data (refs. 4 and 8) also represent $\frac{l}{h}$ values of 1. The improvement (reduction) of the negative base pressure coefficients obtained from the flight application of the splitter plate varies between 30 percent and 40 percent. This level of improvement was as large as that obtained from the two-dimensional wind-tunnel model at the higher comparable Mach numbers and was about 12 percent lower than the model results at the lower comparable Mach numbers. The in-flight improvement was expected to be substantially smaller than that experienced with the model because of the higher flight Reynolds numbers and because of the three-dimensionality of the flow about the flight-test fixture. The expectation relative to dimensional effects was based on data such as that in reference 10 (chapter 16, figs. 2 and 11) in which base pressure coefficient values at $M \leq 0.8$ for two classes of shapes are as follows:

(1) airfoils with blunt trailing edges, $C_{p,b} = -0.50$ to -0.57

(2) body of revolution without fins or boattail, $C_{p,b} = -0.16$ to -0.23

Because the flight-test fixture has an aspect ratio of 0.3, it was expected that outboard end effects would preclude even quasi-two-dimensional flow at subsonic speeds. Thus, the flight-test-fixture base pressure coefficients, which range from -0.28 to -0.35 with reference to free-stream conditions and for $M \leq 0.8$, were not expected to be influenced by a splitter plate as much as for a two-dimensional application such as the wind-tunnel-model results of reference 8.

Most aerodynamic surfaces which terminate with blunt bases, such as on lifting-body reentry or future hypersonic vehicles, are likely to be subject to similar end effects. That is, although the stabilizing fins of such vehicles may have higher aspect ratios, the flow at subsonic speeds will not be two-dimensional. Thus, the present results may be representative of the splitter-plate effectiveness which can be obtained at low speeds on some, or parts of, reentry or hypersonic configurations, both with respect to Reynolds number range and the presence of end effects.

The wind-tunnel results of references 4 and 8 are shown in figure 9 to illustrate the effects of lengthening the plate beyond the value of $\frac{l}{h} = 1$. The loss in effectiveness at $\frac{l}{h}$ values somewhat greater than 1 seems to be typical, in that both references show the same tendency though at somewhat different distances from the base. As the plate is extended farther, the base pressure coefficients gradually approach the values for an aft-facing step, which is, of course, the limit of splitter-plate effectiveness for two-dimensional flow.

It thus becomes apparent that a relatively short splitter plate, $\frac{l}{h} = 1$, provides a large portion of the drag reduction provided by longer devices. This fact is encouraging in that a splitter plate of $\frac{l}{h} = 1$ is structurally feasible for flight applications whether it is a fixed or a retractable-extendable device.

Figure 10 is presented to show how specific reductions in negative base pressure coefficient, such as experienced during this study, can significantly influence the zero-lift drag coefficient of blunt-based aircraft. A portion of the figure has been shaded, between 0.23 and 0.87 on the abscissa, to illustrate the wide range of $\frac{C_{D,b}}{C_{D,0}}$ experienced in flight by two different blunt-based aircraft at significantly different subsonic Mach numbers (refs. 14 and 16). It is apparent that for the X-15 airplane the $C_{D,0}$ level would be reduced by about 15 percent even if the splitter-plate effectiveness were only half that demonstrated during this study.

CONCLUDING REMARKS

A subsonic flight experiment has been conducted to evaluate the effectiveness of a splitter plate in reducing the base drag of a blunt trailing edge fin-like shape. The results, which represent chord Reynolds numbers up to 36.2×10^6, show that the splitter plate, which extended into the wake region a distance of 1 base width, reduced the negative base pressure coefficients between 30 percent and 40 percent. This

increment in base pressure coefficient was as large as obtained on a two-dimensional wind-tunnel model at the higher comparable Mach numbers and about 12 percent lower at the lower comparable Mach numbers, even though the flight results represented higher Reynolds numbers and contained outboard end (three-dimensional) effects.

Flight Research Center,
National Aeronautics and Space Administration,
Edwards, Calif., January 31, 1967,
126-16-05-02-24.

REFERENCES

1. Roshko, Anatol: On the Development of Turbulent Wakes From Vortex Streets. NACA Rept. 1191, 1954.

2. Roshko, Anatol: On the Drag and Shedding Frequency of Two-Dimensional Bluff Bodies. NACA TN 3169, 1954.

3. Roshko, Anatol: On the Wake and Drag of Bluff Bodies. J. Aeron. Sci., vol. 22, no. 2, Feb. 1955, pp. 124-132.

4. Bearman, P. W.: Investigation of the flow behind a two-dimensional model with a blunt trailing edge and fitted with splitter plates. J. Fluid Mech., vol. 21, part 2, Feb. 1965, pp. 241-256.

5. Seban, R. A.; and Levy, A. M.: The Effect of a Downstream Splitter Plate on the Heat Transfer From a Circular Cylinder Normal to an Air Stream. Tech. Rep. 57-479 (ASTIA No. AD 155765), Wright Air Dev. Center, U. S. Air Force, Aug. 1957.

6. Arie, Mikio; and Rouse, Hunter: Experiments on two-dimensional flow over a normal wall. J. Fluid Mech., vol. 1, part 2, July 1956, pp. 129-141.

7. Butsko, J. E.; Carter, W. V.; and Herman, W.: Development of Subsonic Base Pressure Prediction Methods. Tech. Rep. AFFDL-TR-65-157, vols. I and II, Wright-Patterson Air Force Base, U. S. Air Force, Sept. 1965.

8. Nash, J. F.; Quincey, V. G.; and Callinan, J.: Experiments on Two-Dimensional Base Flow at Subsonic and Transonic Speeds. NPL Aero Rep. 1070, British A. R. C., Jan. 21, 1963.

9. Nash, J. F.: A Discussion of Two-Dimensional Turbulent Base Flows. NPL Aero Rep. 1162, British A. R. C., July 20, 1965.

10. Hoerner, Sighard F.: Fluid-Dynamic Drag. Pub. by the author (148 Busteed, Midland Park, N. J.), 1958.

11. Cubbage, James M., Jr.: Jet Effects on Base and Afterbody Pressures of a Cylindrical Afterbody at Transonic Speeds. NACA RM L56C21, 1956.

12. Salmi, Reino J.: Experimental Investigation of Drag of Afterbodies With Exiting Jet at High Subsonic Mach Numbers. NACA RM E54I13, 1954.

13. Mechtly, E. A.: The International System of Units — Physical Constants and Conversion Factors. NASA SP-7012, 1964.

14. Horton, Victor W.; Eldredge, Richard C.; and Klein, Richard E.: Flight-Determined Low-Speed Lift and Drag Characteristics of the Lightweight M2-F1 Lifting Body. NASA TN D-3021, 1965.

15. Saltzman, Edwin J.: Base Pressure Coefficients Obtained From the X-15 Airplane for Mach Numbers Up to 6. NASA TN D-2420, 1964.

16. Saltzman, Edwin J.; and Garringer, Darwin J.: Summary of Full-Scale Lift and Drag Characteristics of the X-15 Airplane. NASA TN D-3343, 1966.

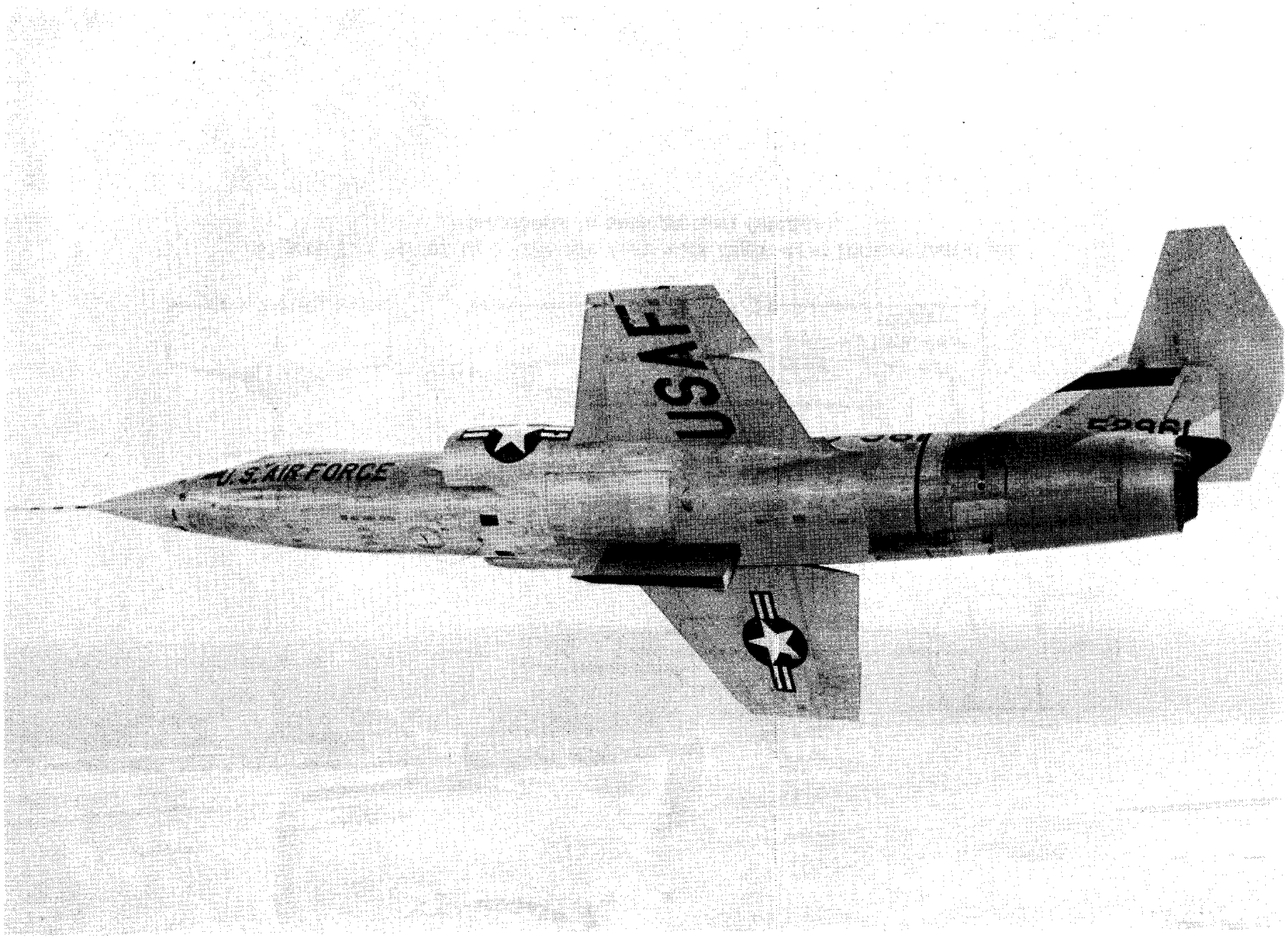

Figur – F-104 airplane with flight-test fixture installed. ECN-714

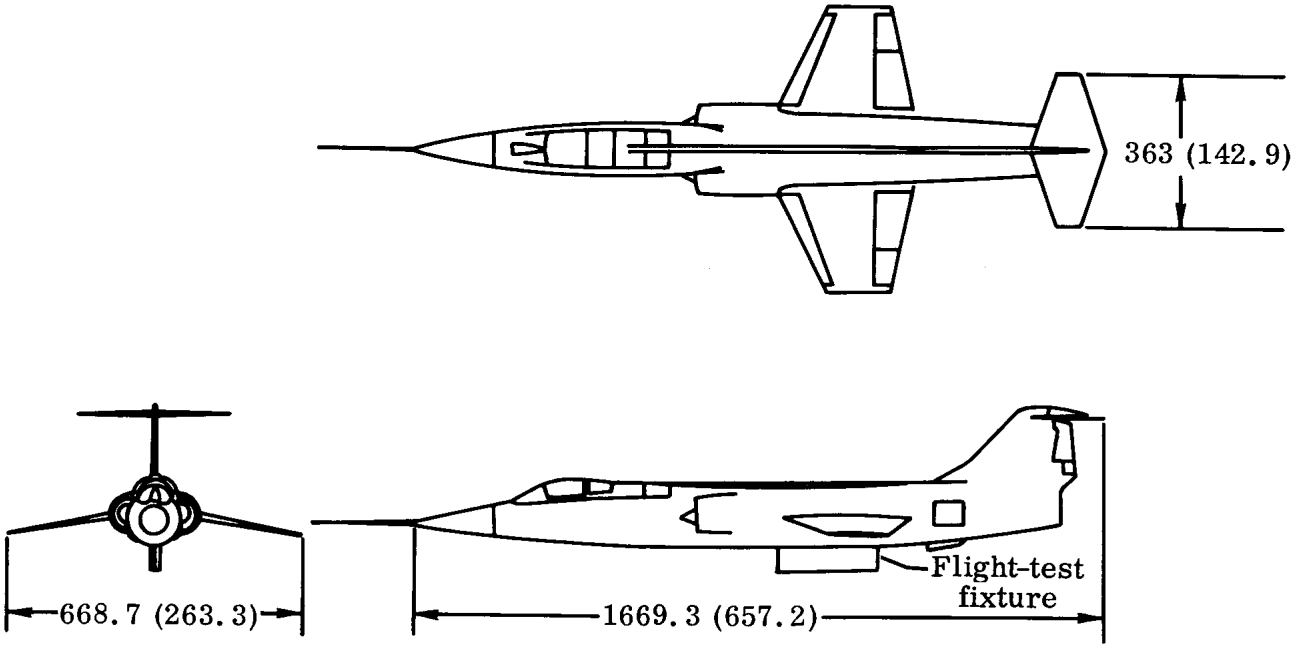

Figure 2. – Sketch of F-104 airplane with flight-test fixture installed.
Dimensions in centimeters (inches).

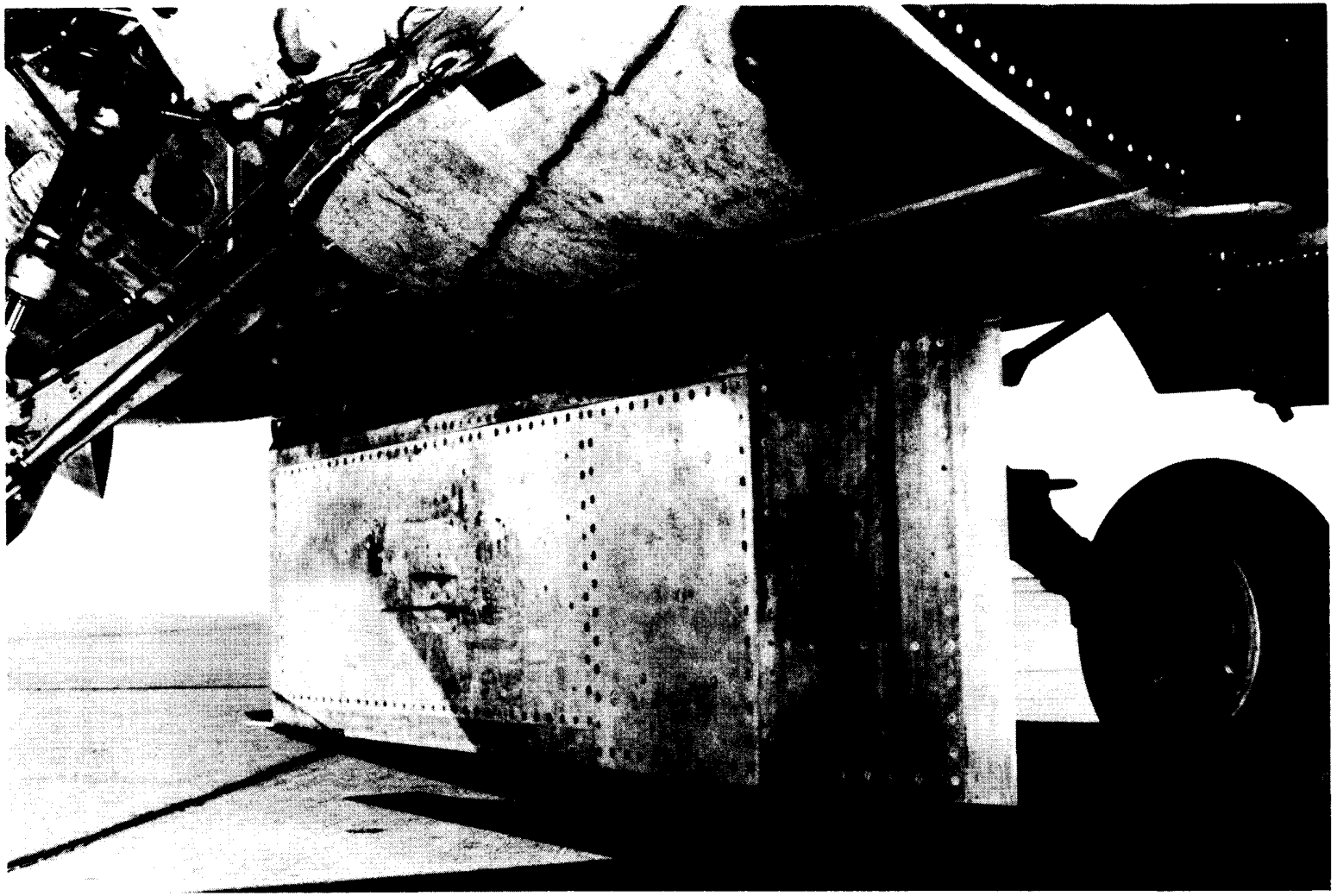

(a) View from 2 o'clock position. (Vertical strip behind leading edge is boundary-layer trip.)

Figure 3. – Photographs of the flight-test fixture.

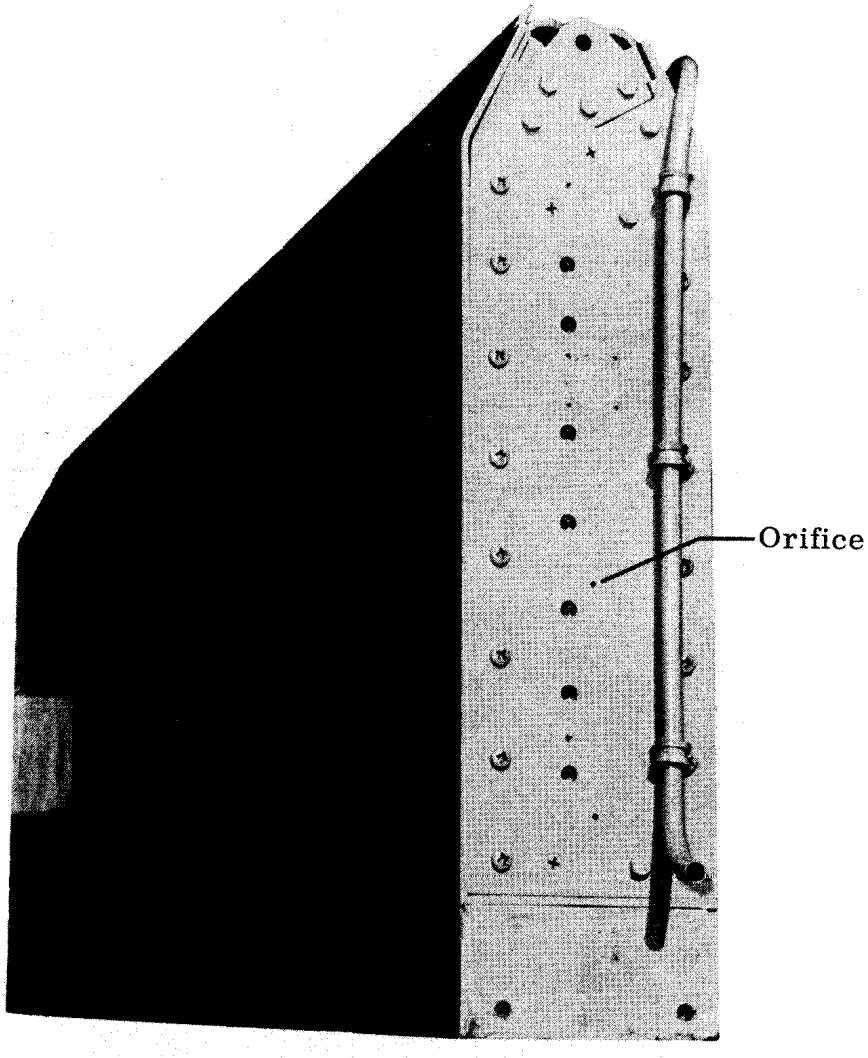

E-16288

(b) View of flight-test fixture base region. (Descending pipe is aircraft fuel-tank vent.)

Figure 3. – Concluded.

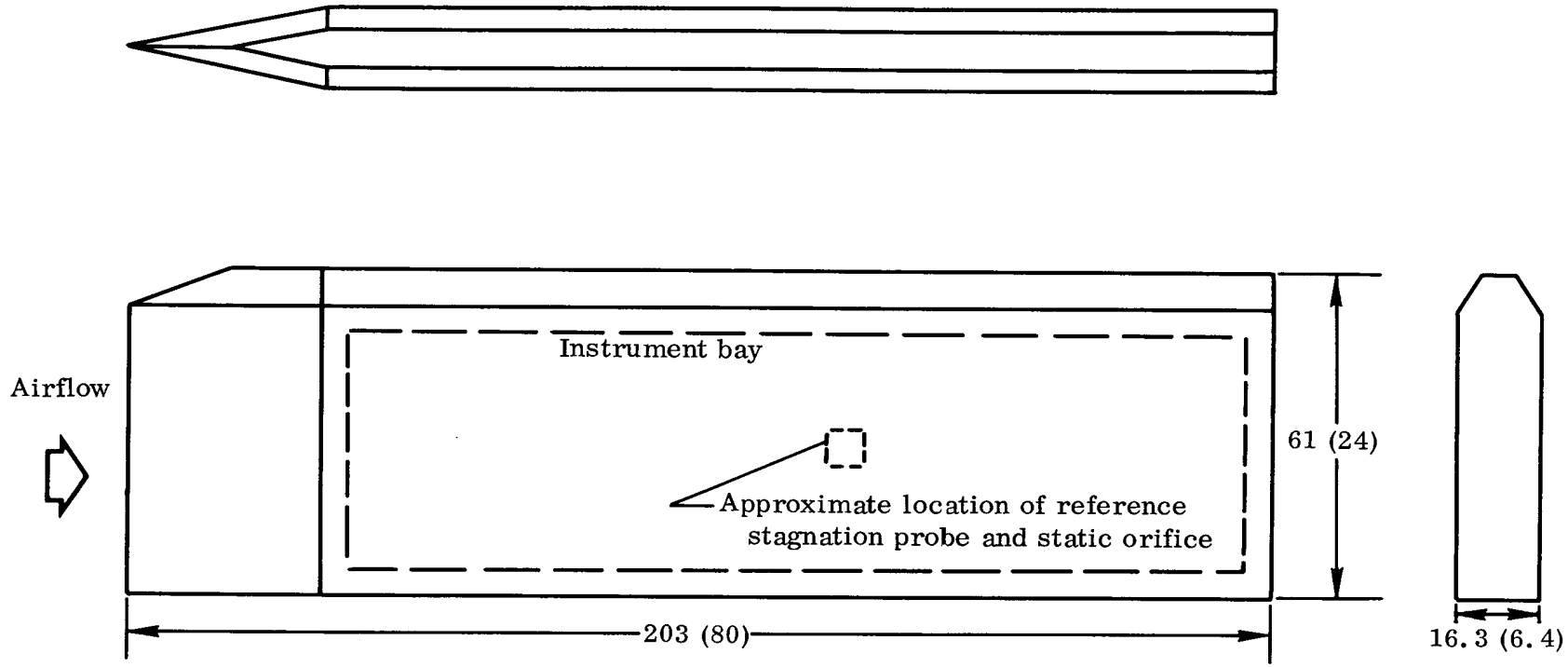

Figure 4. – Sketch of flight-test fixture. Dimensions in centimeters (inches).

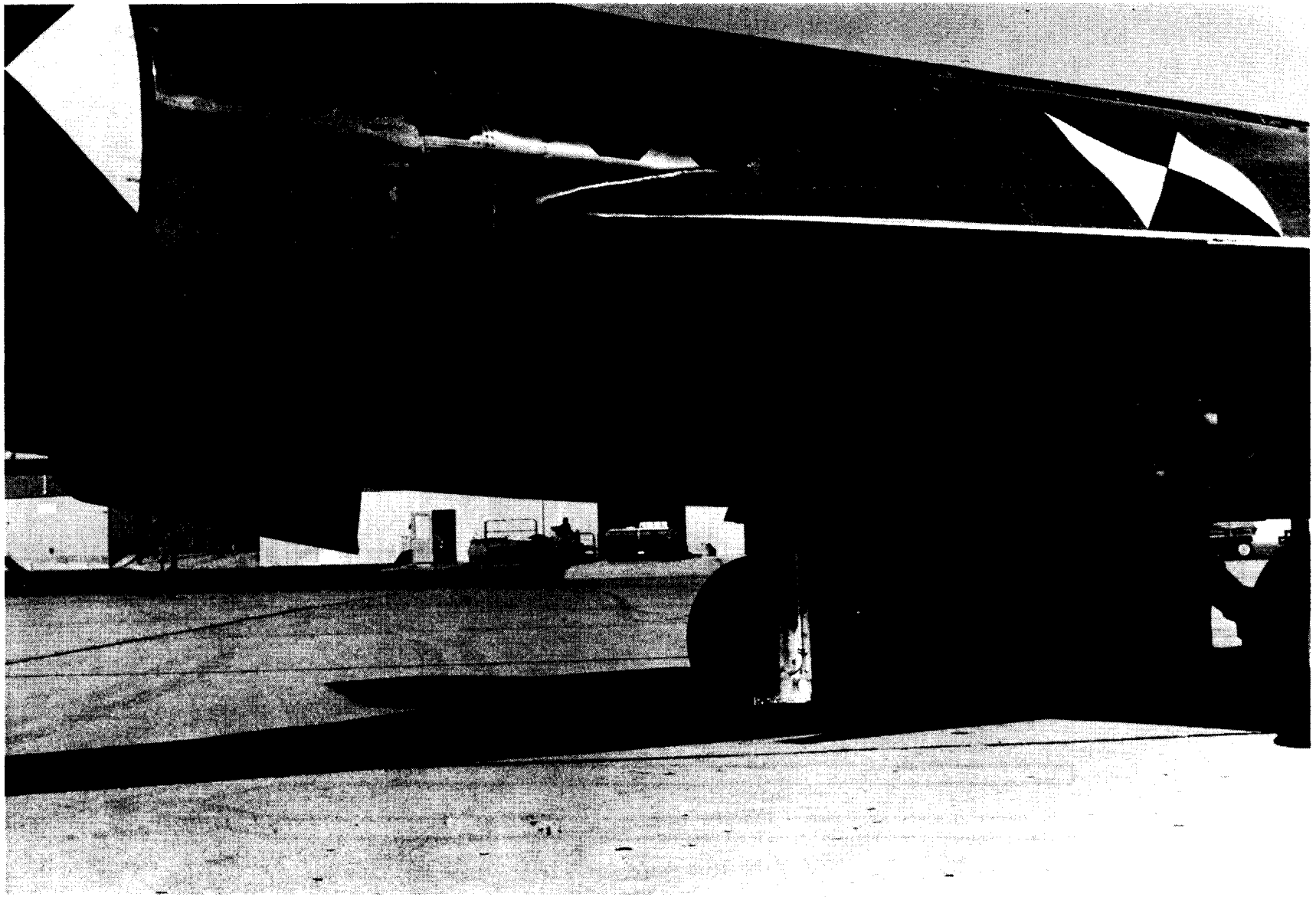

(a) View after installation on F-104 showing portion of aircraft ventral fin removed. ECN-1273

Figure 5. – Flight-test fixture with splitter plate installed.

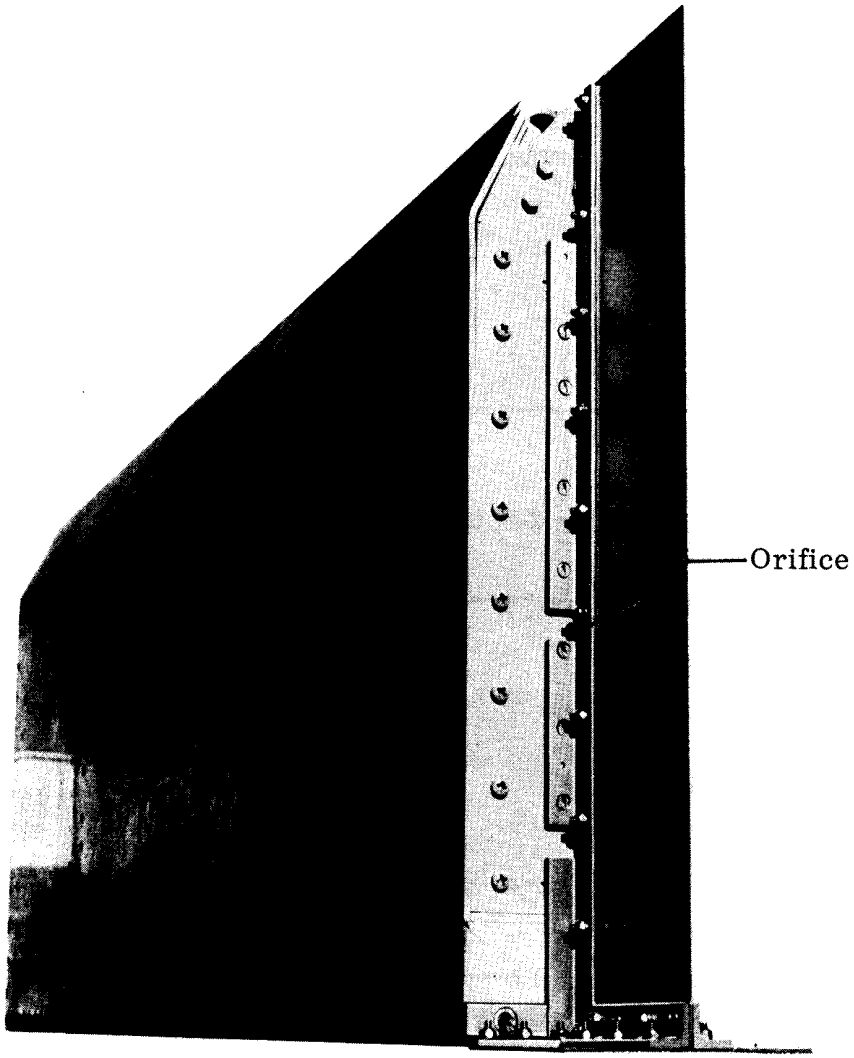

E-16289

(b) Close up view of base with splitter plate.

Figure 5. – Concluded.

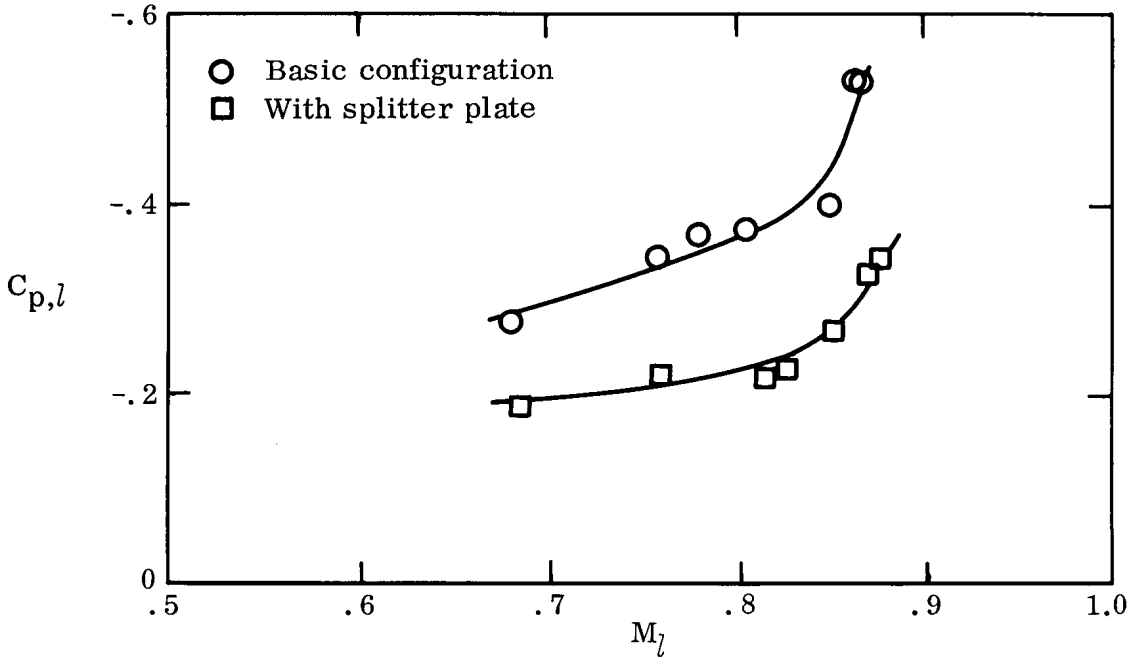

(a) Local reference conditions.

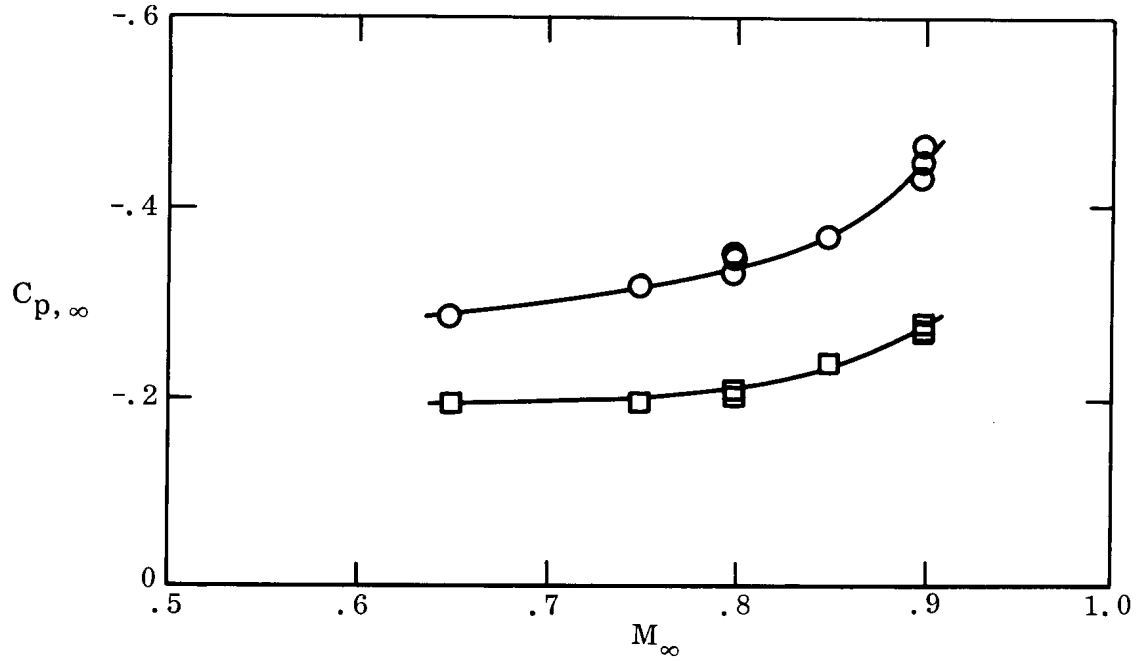

(b) Free-stream reference conditions.

Figure 6. – Flight variation of test-fixture base pressure coefficient with Mach number. Turbulent flow.

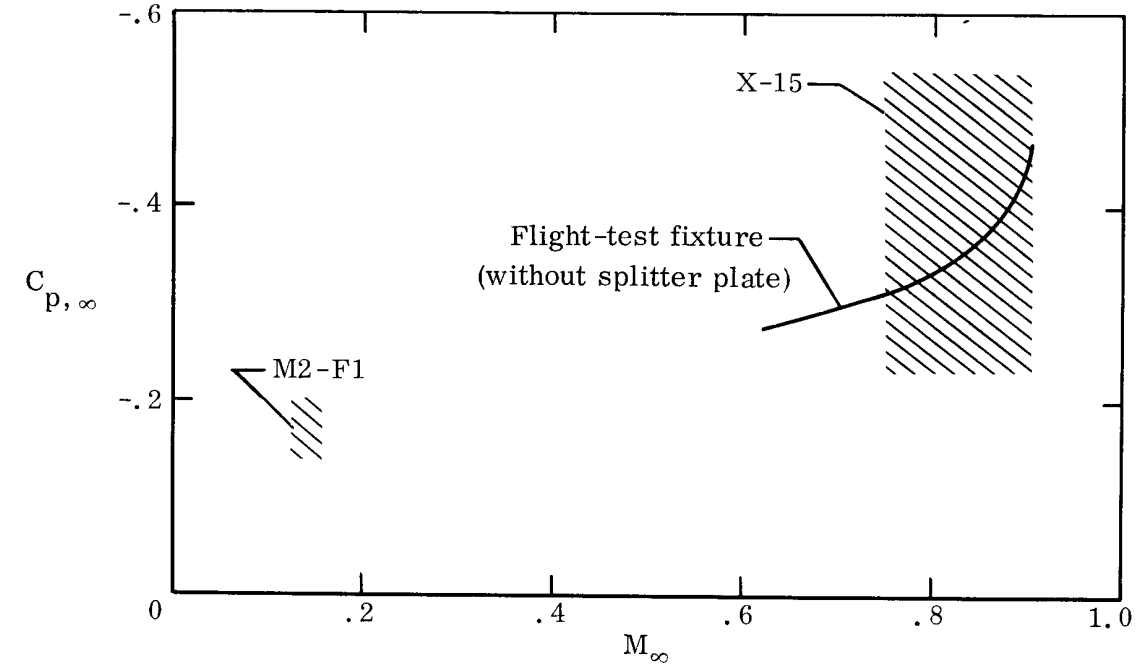

Figure 7. – Comparison of base pressure coefficients from the flight-test fixture with flight results from fins and fin-like projections of two aircraft. Turbulent flow.

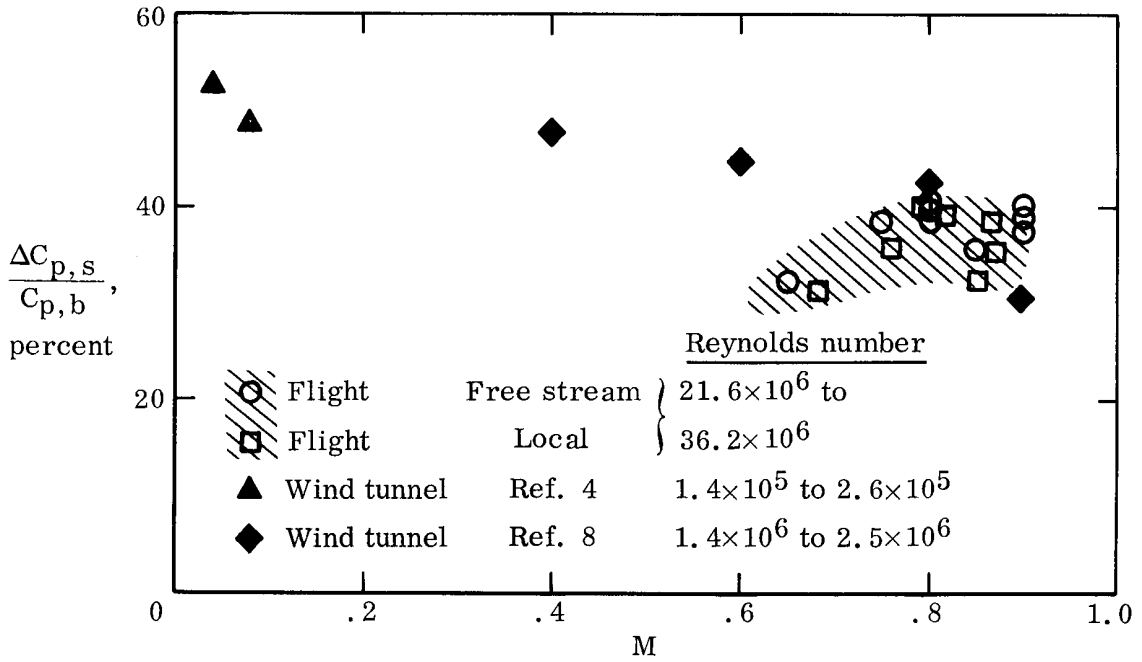

Figure 8. – Comparison of reduction of negative base pressure coefficient obtained in flight with two-dimensional wind-tunnel results. Turbulent flow, $\frac{l}{h} = 1$.

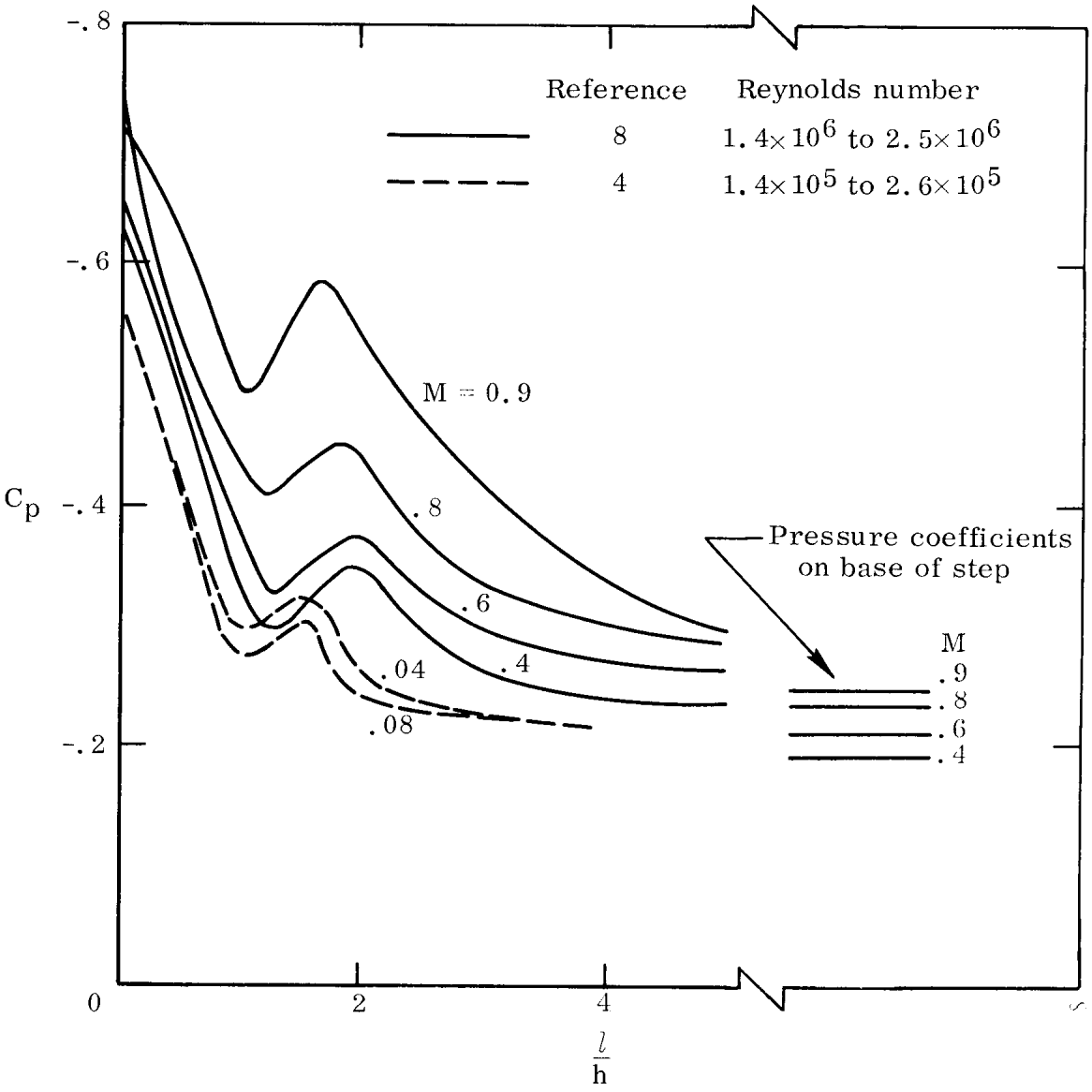

Figure 9.– Effect of length of splitter plate on base pressure in wind-tunnel tests. Turbulent flow.

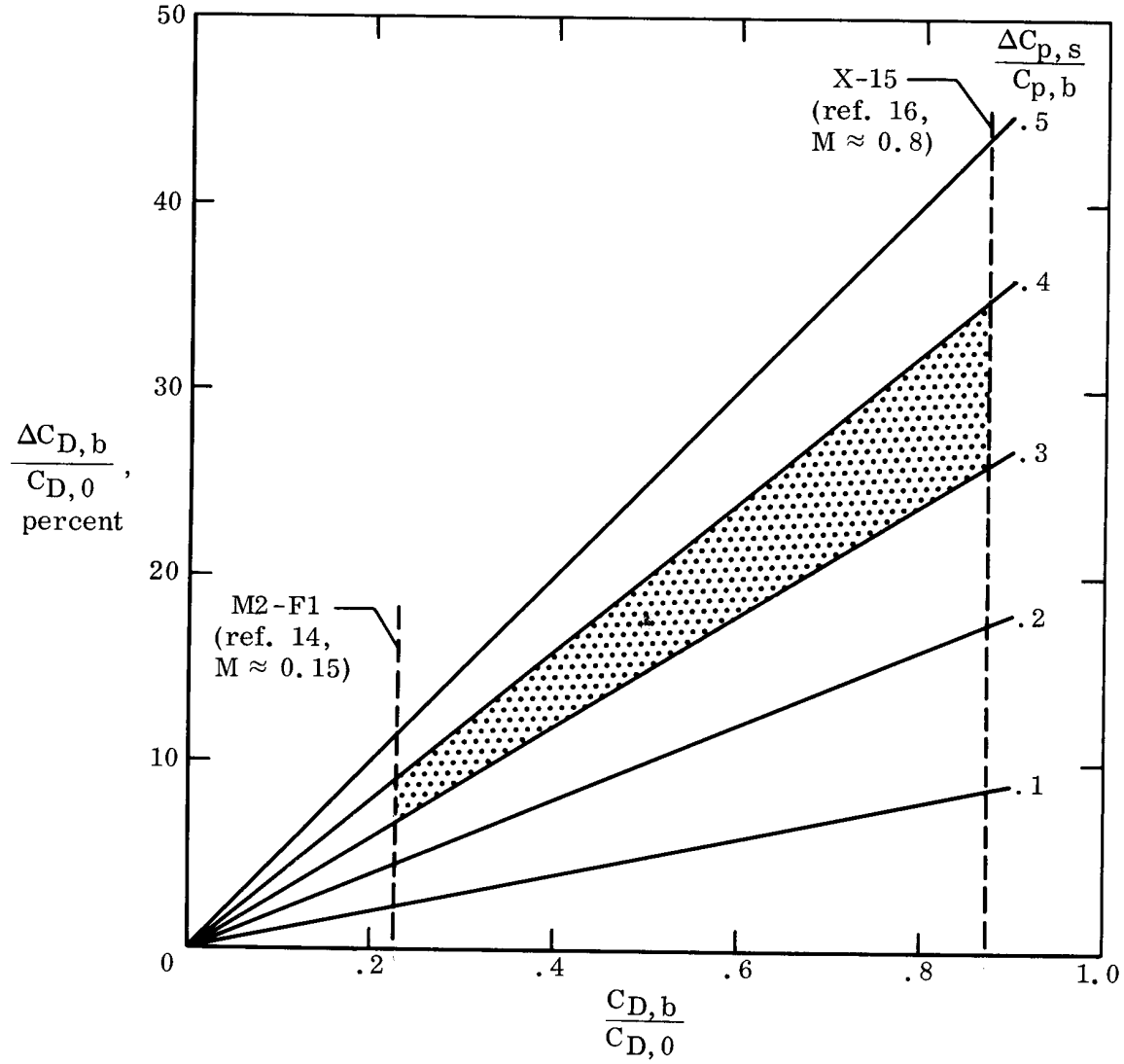

Figure 10. – Calculated effect of splitter-plate benefits on $C_{D,0}$ of hypothetical aircraft for various degrees of base pressure coefficient improvement.